Bioorganic & Medicinal Chemistry 19 (2011) 631–641

Contents lists available at ScienceDirect

Bioorganic & Medicinal Chemistry

journal homepage: www.elsevier.com/locate/bmc

Hypericins and thioredoxin reductase: Biochemical and docking studies disclose the molecular basis for effective inhibition by naphthodianthrones

Francesca Sorrentino [a], Anastasia Karioti [b], Paola Gratteri [c], Maria Pia Rigobello [a], Guido Scutari [a], Luigi Messori [d], Alberto Bindoli [e,*], Matteo Chioccioli [c], Chiara Gabbiani [d], Maria Camilla Bergonzi [b], Anna Rita Bilia [b,*]

[a] Department of Biological Chemistry, University of Padova, Viale G. Colombo 3, 35121 Padova, Italy
[b] PHYTOLAB, Department of Pharmaceutical Sciences, University of Florence, via Ugo Schiff 6, Polo Scientifico, Sesto Fiorentino, 50019 Florence, Italy
[c] Laboratory of Molecular Modeling, Cheminformatics & QSAR. Dipartimento di Scienze Farmaceutiche, via Ugo Schiff 6, Polo Scientifico, Sesto Fiorentino, 50019 Florence, Italy
[d] Laboratory of Metals in Medicine (METMED), Department of Chemistry, University of Florence, via della Lastruccia 3, Polo Scientifico, Sesto Fiorentino, 50019 Florence, Italy
[e] Institute of Neuroscience (CNR), Padova c/o Department of Biological Chemistry, University of Padova, Viale G. Colombo 3, 35121 Padova, Italy

ARTICLE INFO

Article history:
Received 6 July 2010
Revised 14 October 2010
Accepted 16 October 2010
Available online 25 October 2010

Keywords:
Antitumor agents
Anthranoids
Hypericin and pseudohypericin
Glutathione reductase
Thioredoxin reductase
Molecular modeling

ABSTRACT

Cytosolic (TrxR1) and mitochondrial (TrxR2) thioredoxin reductases experience pronounced concentration- and time-dependent inhibition when incubated with the two naphthodianthrones hypericin and pseudohypericin. Pseudohypericin turned out to be a quite strong inhibitor of TrxR1 (IC_{50} = 4.40 μM) being far more effective than hypericin (IC_{50} = 157.08 μM). In turn, the IC_{50} values measured toward TrxR2 were 7.45 μM for pseudohypericin and 43.12 μM for hypericin. When compared to pseudohypericin, the inhibition caused by hypericin usually required significantly longer times, in particular on TrxR1. These important differences in the inhibitory potencies and profiles were analysed through a molecular modeling approach. Notably, both compounds were found to accommodate in the NADPH-binding pocket of the enzyme. The binding of the two naphthodianthrones to thioredoxin reductase seems to be particularly strong as the inhibitory effects were fully retained after gel filtration. Also, we found that TrxR inhibition by hypericin and pseudohypericin does not involve the active site selenol/thiol motif as confirmed by biochemical and modeling studies. The resulting inhibition pattern is very similar to that produced by the two naphthodianthrones on glutathione reductase. As the thioredoxin system is highly overexpressed in cancer cells, its inhibition by hypericin and pseudohypericin, natural compounds showing appreciable anticancer properties, might offer new clues on their mechanism of action and open interesting perspectives for future tumor therapies.

1. Introduction

Anthranoids (Fig. 1) are natural polyphenol constituents based on the anthracene nucleus and chemically can be described as anthrones, dianthrones, anthraquinones, bisanthraquinones, and naphthoanthraquinones. These constituents are characteristic secondary metabolites widely diffused in nature including plants, bacteria, fungi, lichens, and sponges. Anthranoids are well known for their variegate biological activities and find several pharmaceutical applications such as laxative, antimicrobial, antifungal and antiviral agents but also as antitumor drugs.[1–3]

Among the most promising anthranoids, the structurally related naphthodianthrones hypericin (HYP) and pseudohypericin (PHYP), widely present in the *Hypericum* species, are well known for their relevant antitumor, antiviral and antidepressant properties[4,5] (Fig. 2). Studies are mainly related to hypericin, one of the most potent, naturally occurring, photodynamic agents, able to generate the superoxide anion and a high quantum yield of singlet oxygen that are primarily responsible for its remarkable biological effects. Indeed, the produced ROS stimulate lipid peroxidation and protein cross-linkages associated to the formation of carbonyl products. The prooxidant photoinduced properties of hypericin have been exploited for the photodynamic therapy of cancer (PDT), as hypericin, in combination with light, very effectively triggers apoptosis of cancer cells.[6] In addition, hypericin inhibits several enzymes

Abbreviations: BIAM, biotin-conjugated iodoacetamide; DTNB, 5,5′-dithiobis [2-nitrobenzoic acid]; DTT, dithiothreitol; GR, glutathione reductase; HYP, hypericin; PHYP, pseudohypericin; ROS, reactive oxygen species; TrxR1, cytosolic thioredoxin reductase; TrxR2, mitochondrial thioredoxin reductase.

* Corresponding authors. Tel.: +39 0498276138; fax: +39 0498073310 (A.B.); tel.: +39 0554573708; fax: +39 0554573679 (A.R.B.).
E-mail addresses: alberto.bindoli@bio.unipd.it (A. Bindoli), ar.bilia@unifi.it (A.R. Bilia).

0968-0896/$ - see front matter © 2010 Elsevier Ltd. All rights reserved.
doi:10.1016/j.bmc.2010.10.045

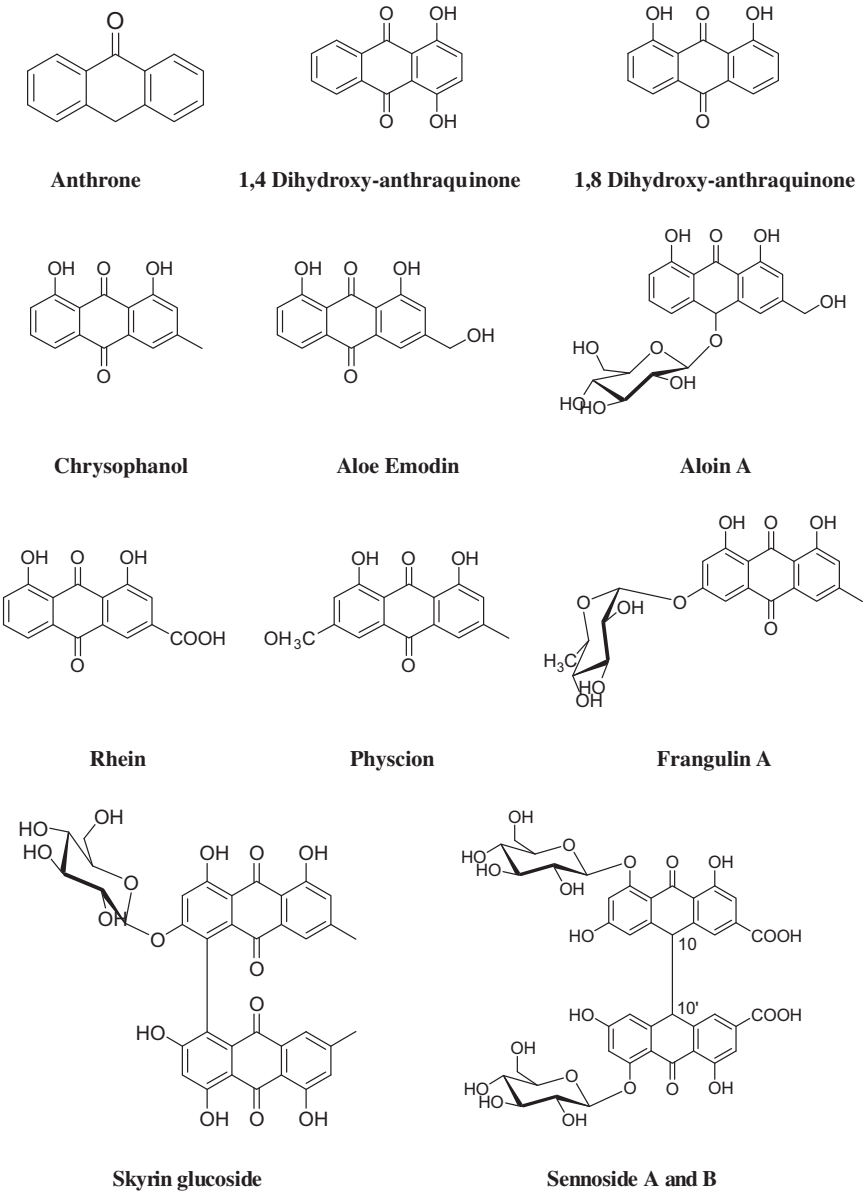

Figure 1. Structures of investigated anthranoids.

such as monoaminooxidase, protein kinase C, cytochrome P-450, telomerase, and reverse transcriptase[4] most of these inhibitions requiring light and oxygen.

The effects of hypericin on the major enzymes acting as antioxidants were studied by Johnson and Pardini,[7] both in tumor cells and on purified enzymes. Cells treated with hypericin and irradiated with fluorescent light show a marked stimulation of the activities of catalase, glutathione peroxidase (GPx), CuZn superoxide dismutase (CuZn SOD), and Mn superoxide dismutase. The latter, in particular, shows a pronounced increase in activity immediately after irradiation. On the contrary, under the same conditions, glutathione reductase was readily inhibited. However, the isolated and purified antioxidant enzymes (GPx, CuZn SOD, and glutathione *S*-transferase (GST) were all inhibited by hypericin in the dark. Among them, the most sensitive was glutathione reductase (GR) that even responded to nanomolar levels of hypericin.[7] Interestingly, and at variance with most of the inhibitory effects reported above, the inhibition of glutathione reductase was observed both after light irradiation and in the dark suggesting that it does not depend on light. Furthermore, with CuZn SOD, GPx, and GST, the inhibitory effects of hypericin decreased in the presence of light, possibly indicating that the interaction of these proteins with hypericin was modified by photoactivation[7] or that the photosensitizer was decomposed. A similar behavior was observed with phosphatidylinositol-3-kinases showing an IC_{50} in the submicromolar range when treated with hypericin.[8] On the contrary, a large number of protein kinases require light irradiation to be inhibited by hypericin.[9]

Both glutathione reductase and thioredoxin reductase are homodimeric enzymes belonging to the same family of FAD-dependent oxidoreductases.[10] They utilize NADPH as the electron donor. In both enzymes, similar FAD, NADPH, and interface domains are present.[11] Both glutathione reductase and thioredoxin reductase contain a dithiol/disulfide catalytic site close to the N-terminus. However, thioredoxin reductase possesses, at the C-terminus, a flexible and exposed peptide containing the SH/Se^{-} motif that allows the enzyme to react with a variety of electrophilic and chemically unrelated compounds.

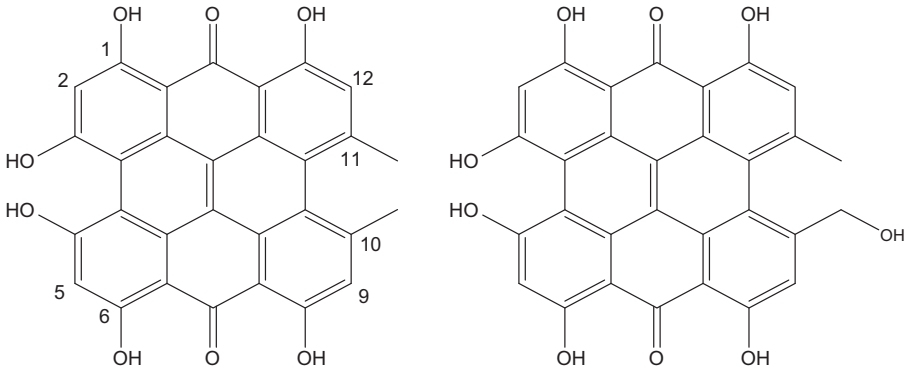

Figure 2. Structures of hypericin and pseudohypericin.

In the present work the effects of several natural anthranoid derivatives, were tested on both cytosolic and mitochondrial thioredoxin reductases, focusing on the naphthodianthrone hypericin and pseudohypericin. We have found that hypericin and, to a greater extent, pseudohypericin act as inhibitors of thioredoxin reductases, both in the dark and in ambient light; moreover, pseudohypericin, similarly to hypericin, also inhibits glutathione reductase. Even more remarkably, MM-GBSA modeling computation performed on the thioredoxin reductase-hypericins system was able to correctly predict the relative binding affinity of hypericins. The consequences of the described inhibitory effects on cell physiology are discussed with particular emphasis on cancer cells.

2. Results

2.1. Inhibition of thioredoxin reductase by the naphthodianthrones hypericin (HYP) and pseudohypericin (PHYP)

In Figure 3 (A and B) the effects of increasing concentrations of HYP and PHYP on the activity of cytosolic and mitochondrial thioredoxin reductase, are reported. As apparent, pseudohypericin markedly inhibits both TrxR1 and TrxR2 with IC_{50} values of 4.40 μM and 7.45 μM, respectively, showing a more pronounced inhibitory effect on the cytosolic isoform. HYP is less efficient than PHYP in inhibiting thioredoxin reductase. HYP appears to be more effective on mitochondrial thioredoxin reductase reaching an IC_{50} value of 43.12 μM which is noticeably lower than that measured for TrxR1 (157.08 μM). The effects of both hypericin and pseudohypericin were also tested on glutathione reductase, as previous research had revealed that hypericin is a potent inhibitor of this enzyme, even in the absence of light irradiation.[7] As apparent from Figure 3C, PHYP inhibits glutathione reductase slightly more efficiently than HYP. Thus, unlike thioredoxin reductases, the two hypericins exhibit minor differences when acting as inhibitors of glutathione reductase (IC_{50} 2.20 and 3.67 μM, for pseudohypericin and hypericin, respectively). However, similarly to TrxRs, PHYP results more effective than HYP. From inspection of Figure 3 (D–F) it clearly emerges that the inhibitory actions of HYP and PHYP are markedly time-dependent. In particular, 20 μM hypericin, after 1 h incubation, is able to inhibit TrxR1 by about 60%, while after 2 min incubation the measured enzyme inhibition is solely of 20%. Moreover, pseudohypericin exhibits a more rapid kinetics of TrxR1 inhibition (a 50% inhibition was indeed achieved after 2 min incubation with 5 μM pseudohypericin). With TrxR2 (Fig. 3E) and glutathione reductase (Fig. 3F) the inhibitory effects of hypericin are slightly more rapid than those observed with TrxR1, while pseudohypericin shows an efficiency comparable to that found for TrxR1.

Results of Fig. 3 were obtained using the artificial substrate DTNB as electron acceptor in the TrxR assay. The inhibitory effects of HYP and PHYP on TrxRs were further confirmed by using the insulin assay method (Fig. 4). In this assay, thioredoxin, reduced at expenses of NADPH, in turn reduces insulin that precipitates and gives rise to a marked turbidity. Therefore, in the first phase of the process, the enzyme activity could be followed as a decrease of absorbance; subsequently, the increase of turbidity was monitored (See Fig. 4, control). With HYP the rate of absorbance decrease is slightly lower than control; thus, the turbidity starts increasing, after about 13 min (TrxR1) or 23 min (TrxR2) (Fig. 4). In contrast, with PHYP, the oxidation of NADPH is very small and no turbidity appears over 30 min observation in the presence of either TrxR1 or TrxR2. Comparing the results shown in Fig. 4 with those of Fig. 3, it is confirmed that PHYP strongly inhibits both TrxR1 and TrxR2, while HYP shows a less marked inhibitory effect.

The results obtained with the insulin method also rule out any interference of the detection reagent DTNB—or of its reduced forms—with the two naphthodianthrones. We have further examined the inhibitory properties of HYP and PHYP by directly following the reduction of Trx in the absence of insulin. As apparent from Fig. 5, no reaction occurs between NADPH and HYP and PHYP. Further addition of TrxR1, in the absence of Trx, gives rise only to a very low decrease of absorbance with time indicating that hypericins are not directly reduced by thioredoxin reductase. Sequential addition of oxidized Trx elicits a sharp decrease of absorbance in the control, which, however, is slower in the presence of hypericin. With pseudohypericin, no stimulation of enzyme activity occurs at all.

2.2. Effect of different redox conditions on the inhibitory effects of HYP and PHYP on thioredoxin reductase

As most organic molecules interact with thioredoxin reductase at the SH/Se^- motif, we explored if HYP and PHYP too might specifically target the reactive C-terminus of thioredoxin reductase. As the enzyme undergoes a reversible redox transition from the SH/Se^- to S-Se state during its catalytic cycle, TrxR1 was treated with hypericins both in the oxidized (S-Se) and in the reduced (SH/Se^-) form. After gel chromatography, necessary to get rid of the excess reagent, it is apparent (Fig. 6) that TrxR1, treated with 100 μM HYP or PHYP, both in oxidizing (−NADPH) and reducing (+NADPH) conditions, is moderately inhibited by hypericin and markedly inhibited by PHYP, indicating that inhibition is largely independent on the interaction with the active site thiol/selenol

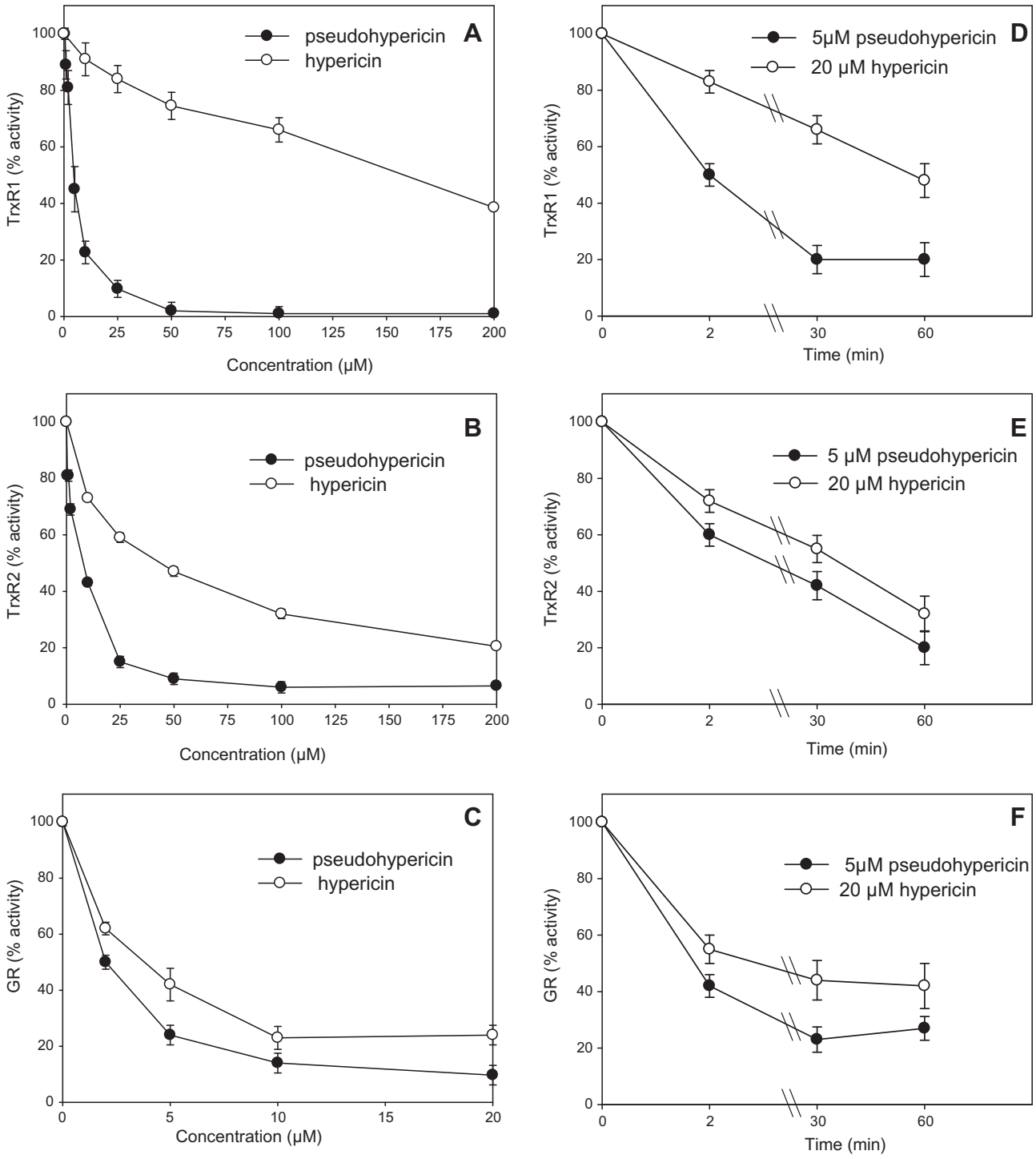

Figure 3. Concentration and time-dependent inhibitory effect of HYP and PHYP on cytosolic and mitochondrial thioredoxin reductase and on yeast glutathione reductase. Cytosolic (TrxR1, A) and mitochondrial (TrxR2, B) thioredoxin reductase (1–3 μg/ml) were incubated for 5 min at 25 °C in 0.2 M Na, K-phosphate buffer (pH 7.4) containing 0.25 mM NADPH, 2 mM EDTA and increasing concentrations of hypericin or pseudohypericin. Reactions were started by the addition of 1 mM DTNB and followed spectrophotometrically at 412 nm. (C) Inhibitory effect of hypericin or pseudohypericin on yeast glutathione reductase (GR). Glutathione reductase (0.8 μg/ml) activity was assayed at 25 °C in 0.1 M Tris-HCl buffer (pH 8.1) containing 0.2 mM NADPH and increasing concentrations of HYP or PHYP. After 5 minutes of incubation, reactions were started by the addition of 1 mM GSSG and followed spectrophotometrically at 340 nm. Thioredoxin reductases (D, E) and glutathione reductase (F) were incubated as before for 2, 30 and 60 minutes in the presence of 20 μM HYP or 5 μM PHYP and the reactions initiated by the addition of 1 mM DTNB for thioredoxin reductases and 1 mM GSSG for glutathione reductase and followed at 412 and 340 nm, respectively.

residues. In addition, the persistence of the inhibitory effect, even after two sequential chromatographic steps, indicates that the binding of HYP and PHYP to the enzyme is very strong. Later on, the results of gel filtration chromatography tests were confirmed by experiments where both TrxRs, after treatment with HYP and PHYP, were extensively dialyzed. As it is evident from the inset to Fig. 6A, the inhibitory effects, particularly of PHYP, are retained after dialysis; in addition, the extent of the observed inhibition is in good agreement with the values reported in Fig 3A and B. The limited interaction of HYP and PHYP with thiol/selenol groups of

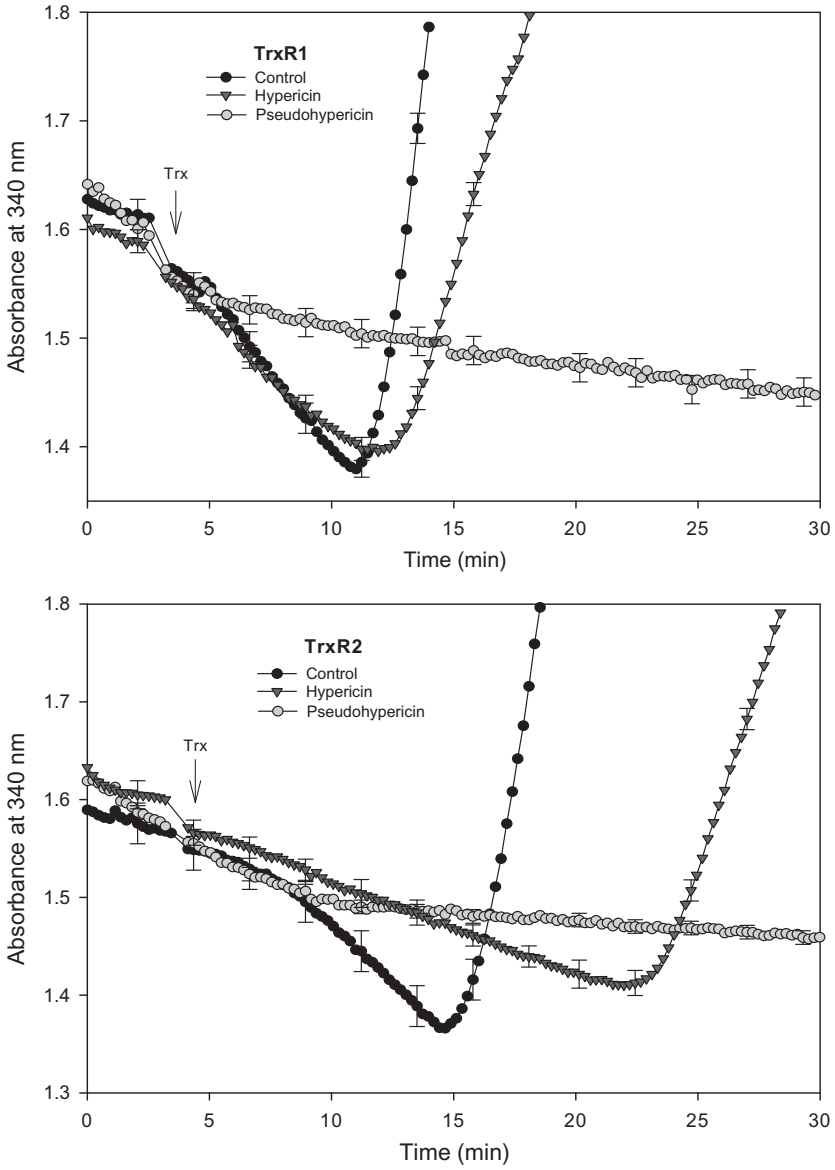

Figure 4. Inhibition of cytosolic and mitochondrial thioredoxin reductases by HYP and PHYP estimated with the insulin reduction method. TrxR1 (2–3 μg/ml) was incubated for 5 minutes at 25 °C in 0.2 M Na, K-phosphate buffer (pH 7.4) containing 0.25 mM NADPH, 0.17 mM insulin, 2 mM EDTA and, where indicated, 100 μM HYP or PHYP. The reaction was started by the addition of 10 μM *E. coli* thioredoxin (Trx, at the arrow) and followed spectrophotometrically at 340 nm.

thioredoxin reductase was further confirmed by experiments with BIAM (Fig. 6B) indicating that the SH/Se^- motif is scarcely modified at low pH (6.5), a condition that allows the reactivity of only selenol and the 'reactive' (low pK_a) thiols. The lack of effect on the C-terminus of thioredoxin reductase is fully consistent with the observed inhibition of glutathione reductase.

2.3. Molecular modeling

From a structural point of view both cytosolic (TrxR1) and mitochondrial (TrxR2) mammalian thioredoxin reductases are dimers formed by two identical subunits ('homodimers') faced each other by the interface domain in a 'head-to-tail' arrangement. Here, the C-terminal tail of one subunit interacts with the active site of the N-terminal opposing subunit. Two other domains, named FAD-binding domain and the co-factor NADPH-binding domain, complete the description of the subunit structure. Sequence (Fig. 7) and three dimensional (Fig. 8) alignments of TrxR1 (1h6v) and TrxR2 (1zdl) homodimers allow to highlight non-conserved residues in the two proteins and to appreciate the overall comparable structural architecture of the two enzymes. Notably, all docking experiments carried out on TrxR1 and TrxR2 identify the binding domain for NADPH as the common binding pocket for the exogenous ligands HYP and PHYP, thus confirming the biochemical results concerning the independence of the HYP and PHYP inhibitory action from any interaction with the active site thiol/selenol residues. Scoring functions usually employed by docking programs to energetically evaluate large ensembles of molecules over a short period of time, answer to speed processing criteria that lead to inaccuracy in predicting the free binding energy due to many approximations, such as inadequate treatment of solvation and lack of protein flexibility.[12]

Because the solvent can have a major effect on energies, especially in molecules such as the here studied natural ligands bearing several polar functional groups, and in order to study the association of the ligands with the receptor further, prepositioned selected

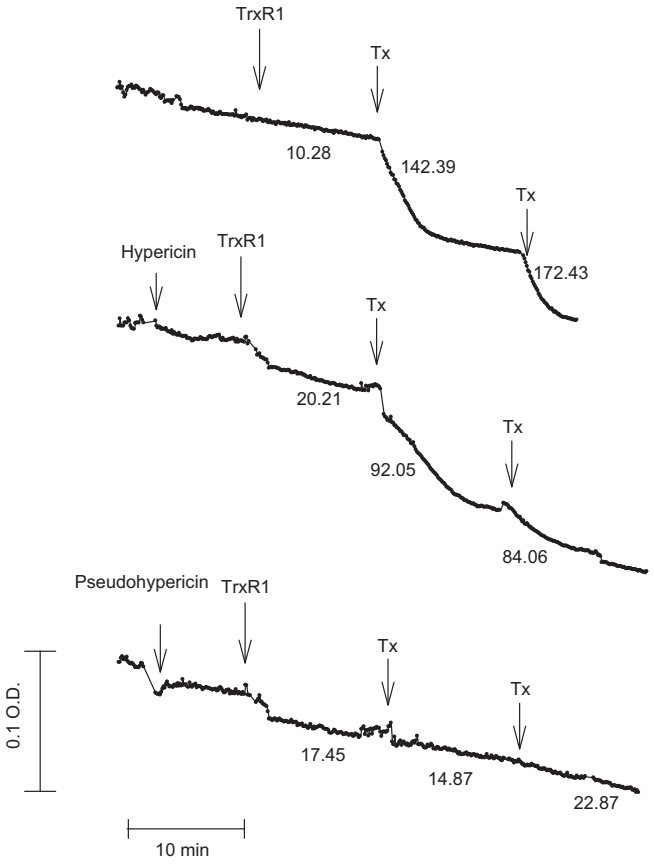

Figure 5. Comparative effect of HYP and PHYP on rat liver cytosolic thioredoxin reductase utilizing thioredoxin in the absence of insulin. Incubations were carried out at 25 °C in 0.2 M Na, K-phosphate buffer (pH 7.4) containing 0.25 mM NADPH and 2 mM EDTA. Where indicated, 50 μM HYP or PHYP were also added. At the indicated times 2 μg thioredoxin reductase (TrxR1) and 10 μM *E. coli* thioredoxin (Trx) were sequentially added. Numbers by the curves indicate TrxR1 activities in nmoles/ min/ mg protein.

poses of hypericin and pseudohypericin coming from docking were submitted to an MM-GBSA procedure for calculating ligand binding energies within a GB/SA continuum solvation model.[13]

The poses were minimized, in turn, with the receptor and energy changes upon association were estimated. The docked poses of both HYP and PHYP in TrxRs enzymes are engaged in a H-bond network and their polycyclic moieties are in good van der Waals contacts with the TrxR2 residues Y228(Y200)—in parenthesis the corresponding residues in TrxR1—L253(L225), F256(F228) G255(G227), K340(K315), S227(S199) (Fig. 9). The predicted ΔG binding energies for hypericin and pseudohypericin reported in Table 1 point out the ability of the MMGB/SA score to discern the differences in the experimental IC_{50} values, the HYP versus PHYP ΔG binding ratio reflecting the HYP versus PHYP pIC_{50} ratio for both TrxRs enzymes.

2.4. Kinetic analysis of the inhibition of TrxR1 by pseudohypericin

From the molecular modeling studies it is clearly apparent that the exogenous ligands HYP and PHYP bind in close proximity to the domain for NADPH. Taking into account this finding, kinetic analysis at increasing concentrations of NADPH, maintaining DTNB at a fixed concentration, was carried out in the absence and presence of different concentrations of PHYP. As apparent in Figure 10, a Lineweaver–Burk plot (Fig. 10A) shows PHYP inducing a linear mixed-type inhibition further confirmed by plotting the same data in a Dixon (Fig. 10C) or Cornish-Bowden (Fig 10D) plot. In addition to these representations, secondary plots of Fig. 10 A allow the calculation of the dissociation constants for EI complex (K_i) and EIS complex (K'_i) which are in good agreement with the values obtained from the Dixon and Cornish-Bowden plots. As apparent, K_i (1.9 μM) is lower than K'_i (8.1 μM) indicating that the affinity of the enzyme for TrxR1 alone is greater than that for the enzyme–substrate complex. It should also be noted that, in presence of NADPH, thioredoxin reductase shows an appreciable substrate inhibition at concentrations higher than 20 μM. Therefore in a Lineweaver–Burk plot, at relatively high concentrations of NADPH, data points are found above the straight line.[14]

2.5. Thioredoxin reductase inhibition by structurally related compounds

For comparison purposes a panel of compounds bearing the anthranoid structure (see Fig. 1) were challenged against thioredoxin reductases. Their effects on enzyme activities are reported in Table 2. While anthrone and dihydroxyanthraquinones have no effect both on TrxR1 and TrxR2, some major anthraquinones such as those found in rhubarb (chrysophanol, physcion, and rhein) show some moderate inhibitory effects, for instance, rhein exhibits IC_{50} of 84 and 123 μM with TrxR1 and TrxR2, respectively. The effect of rhein toward the cytosolic thioredoxin reductase is superior to that of HYP but, in general, all these compounds appear to be far less effective than PHYP. It is also apparent that the glucoside derivatives of the various anthranoids (aloin A, frangulin A, sennosides A and B, and skyrin glucoside) are almost invariably ineffective in inhibiting both TrxR1 and TrxR2.

3. Discussion and conclusions

The thioredoxin system—formed by NADPH, thioredoxin reductase and thioredoxin—plays a variety of functional roles in the cell, going from the control of the redox balance to synthesis of deoxyribonucleotides and prevention of oxidative stress.[15] In particular, this system is overexpressed in cancer cells and, on this ground, there is an active search for inhibitors of both thioredoxin or thioredoxin reductase. Consequently, thioredoxin reductase has recently become an important target in tumor drug therapy and a great deal of compounds was indeed found capable of inhibiting this enzyme.[16] Among them, several natural quinones and polyphenols such as curcumin and flavonoids were shown to act as strong inhibitors of TrxR by interacting with the active site thiol/selenol group.[17–19] Some quinones are also able to inhibit TrxR by activating a redox cycling process.[20] Antitumor anthracyclines were shown to generate superoxide in the presence of thioredoxin reductase in a reaction reinforced by the presence of thioredoxin, indicating that the whole thioredoxin system is involved in the generation of ROS.[21] However, in a subsequent work,[22] it was reported that anticancer anthracyclines such as daunorubicin and doxorubicin act as poor substrates of thioredoxin reductase and, in addition, are not able to inhibit this enzyme.

Many anthranoids display anticancer properties and therefore can be of potential therapeutic interest,[23] however, no extensive studies of the effects of these compounds on thioredoxin reductase and the thioredoxin system are available so far. In the present paper, the action on thioredoxin reductase of two representative naphthodianthrones, is reported. We have shown that HYP and, to a greater degree, PHYP, are indeed effective inhibitors of both cytosolic and mitochondrial thioredoxin reductases with an effect that is both time- and concentration-dependent (Fig. 3). PHYP

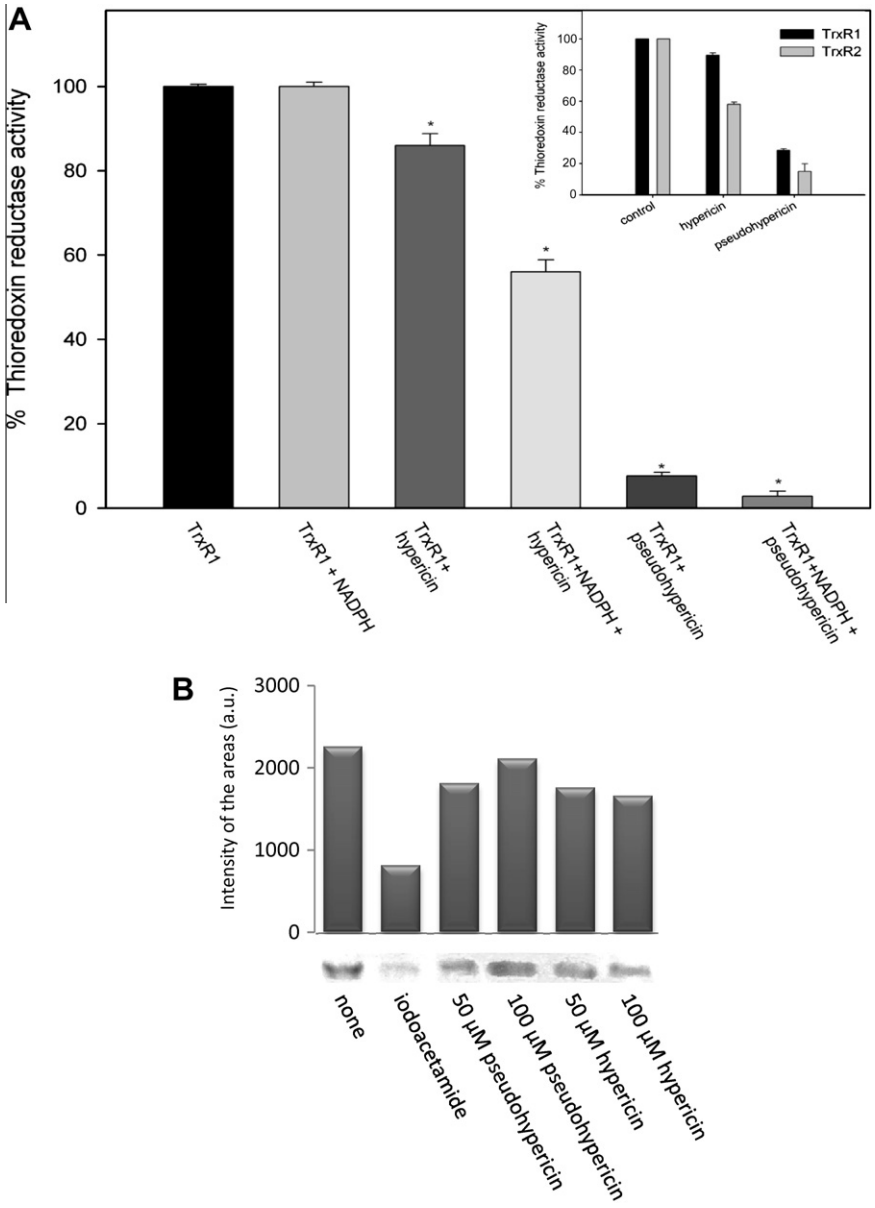

Figure 6. Binding of HYP and PHYP on thioredoxin reductases and effect of different redox conditions on their inhibitory action. (A) TrxR1 (0.12 mg/ml) was incubated in 0.2 M Na, K-phosphate buffer (pH 7.4) containing 2 mM EDTA in the absence or presence of 0.025 mM NADPH in a final volume of 45 μl. After 1.5 minutes of preincubation, 100 μM HYP or PHYP were added where indicated and the reaction carried out for further 7 min. Afterwards, samples were applied to a Micro Bio-Spin (Bio-Rad) desalting column and centrifuged at 1,000 × g for 4 minutes. The obtained samples were again applied to new chromatographic columns and the filtration repeated in order to remove any remaining trace of HYP or PHYP. Thioredoxin reductase activity was measured in the filtrated from column with the DTNB method as indicated in the legend to Fig. 3. The inset of (A) reports the effect of HYP and PHYP on thioredoxin reductases after removal of the reagents by dialysis. TrxR1 (0.12 mg/ml) or TrxR2 (0.15 mg/ml) were incubated with 100 μM HYP or PHYP in 10 mM Tris-HCl, 1 mM EDTA (pH 7.4) for 30 min in the dark. Afterwards, samples were extensively dialyzed overnight at 5 °C against the same buffer. Dialyzed samples were assayed with the DTNB procedure as indicated above. (B) Alkylation of TrxR1 with BIAM after treatment with the indicated concentrations of HYP and PHYP.

appears to be particularly efficient on TrxR1. However, at variance with most known inhibitors of thioredoxin reductases, HYP and PHYP do not seem to interact with the active site selenol/thiol motif as both the oxidized and reduced form of the enzyme are inhibited to a similar extent. Previous research had shown that several inhibitors of thioredoxin reductases are unable to inhibit glutathione reductase as they act essentially at the C-terminal portion of the enzyme bearing the thiol/selenol group.[22,24,25] Accordingly, they should be considered as specific reagents for the thiol/selenol motif of thioredoxin reductase. This view is reinforced by the observation that *Escherichia coli* thioredoxin reductase, lacking the C-terminal portion, is not affected by the gold complex auranofin. The latter, on the contrary, inhibits very strongly—even at the nanomolar level—both cytosolic and mitochondrial thioredoxin reductases. Therefore, HYP and PHYP seem to inhibit thioredoxin reductase with a mechanism similar to that of glutathione reductase; the direct molecular comparison between glutathione reductase and thioredoxin reductase could help in understanding the action mechanism of these inhibitors.

HYP and PHYP are very similar from a chemical point of view, the only difference being the presence of a hydroxymethyl group in PHYP that substitutes a methyl group of HYP (Fig. 2) making the former more hydrophilic.[26] As already reported, our docking experiments carried out both on TrxR1 and TrxR2 identify the NADPH domain as the common binding site for HYP and PHYP. The docked orientations assumed by the two bound ligands both

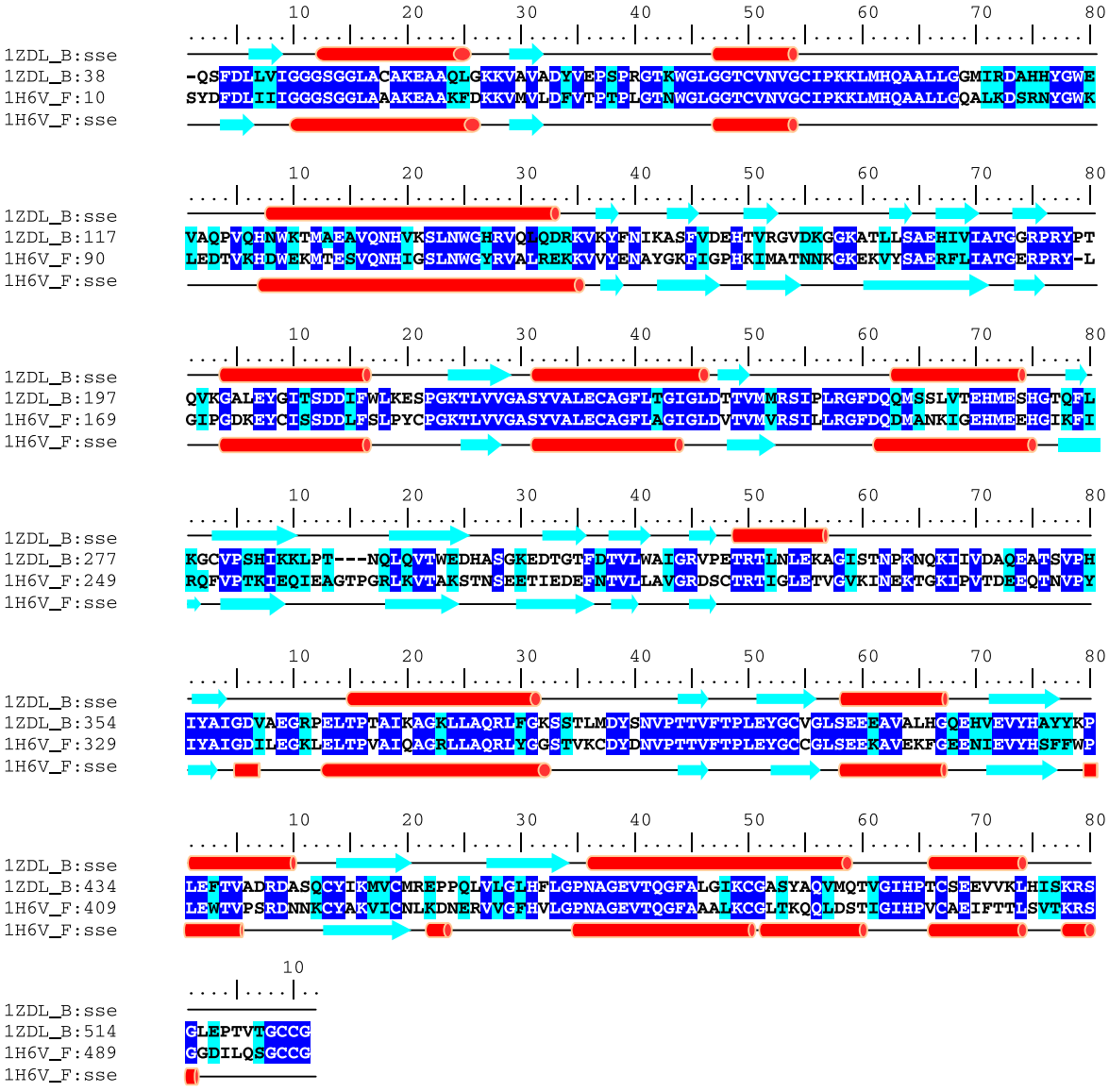

Figure 7. Sequence alignment between TrxR1 (chain F) and TrxR2 (chain B). TrxRs secondary structure is presented on the top of the alignment, where α-helices and ß-strands are represented by red cylinders and cyano arrows, respectively. Conserved and identical amino acid residues are highlighted in cyano and blu, respectively. Sequence numbering is reported right of the sequences.

in TrxR1 and TrxR2 differ from each other due to the facility of their hydroxyl groups to H-bond with the functional groups of the backbone and side chains residues of the two enzymes (Fig. 9). The H-bond network engaged by HYP and PHYP in TrxR2 comprise R254 (HYP and PHYP), E366 (HYP and PHYP), R364 (HYP), R193 (HYP), and S227 (PHYP). As far as TrxR1 is concerned, the residues T372 (HYP), G384 (HYP), V370 (HYP), R226 (PHYP), R293 (PHYP), and R166 (PHYP) were involved. The free binding energies of HYP and PHYP poses were estimated through a MM-GBSA procedure and the measured ΔG value was found to correlate quite satisfactorily with the differences in the enzyme inhibition constants, experimentally determined. Therefore, the modeling results reported here turned out extremely valuable to explain the marked differences observed between HYP and PHYP in their interaction with thioredoxin reductase. These differences in interaction modes apparently arise from the small chemical difference existing between these two molecules. Differences between the two naphthodianthrones in their interactions with proteins were previously reported. For instance, PHYP, in contrast to HYP, strongly binds to some serum components indicating the occurrence of an irreversible interaction.[26] Furthermore, PHYP appears to be up to six times more efficient than HYP in inhibiting a few serine/threonine kinases under similar light conditions.[27] The simultaneous inhibition of the glutathione and thioredoxin systems can have very important consequences for the cell physiology as this condition largely prevents the removal of hydrogen peroxide by glutathione peroxidase and peroxiredoxins. Consequently, the intracellular hydrogen peroxide concentration increases and an unbalance of the redox state of thiols very likely occurs involving thioredoxin, glutathione and glutaredoxin. The latter, was recently shown to play a relevant role in cell proliferation and/or apoptosis.[28] Furthermore, the photoactivating properties of naphthodianthrones could provide a sustained source of ROS. An important feature is that the inhibitory effects on both thioredoxin reductase and glutathione reductase occur both in the dark and in ambient light conditions. This property opens interesting perspectives when considering the potential pharmacological application of these compounds as this specific inhibitory action might reinforce the already well known

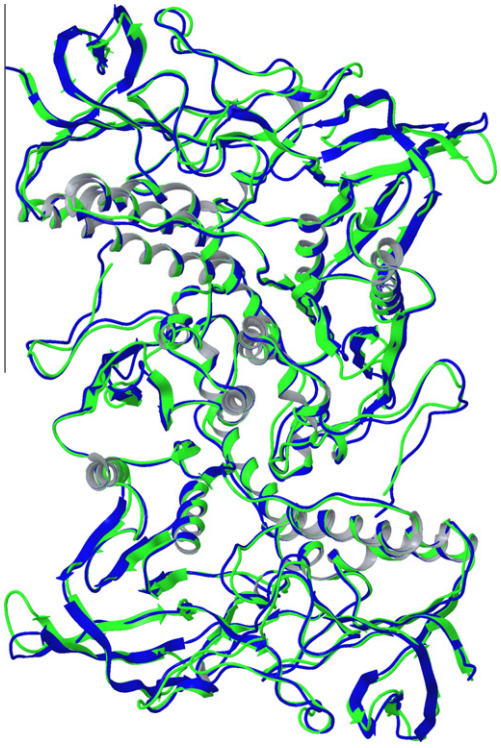

Figure 8. Ribbon representations of the 3D superimposed structures of TrxR1 chain F (blue) and TrxR2 chain B (green).

Table 1
HYP and PHYP experimental pIC_{50} values and binding free energies (in kcal/mol) estimated from MMGB/SA computation in TrxR enzymes

		pIC_{50}	MMGB/SA ΔG
TrxR1	HYP	3.801	−22.24
	PHYP	5.356	−34.61
TrxR2	HYP	4.365	−29.34
	PHYP	5.128	−30.71

photodynamic properties. Moreover, this inhibition might occur even in the absence of oxygen such as in ischemic conditions or in the absence of photoactivating light.

4. Experimental section

4.1. Drugs and Chemicals

All the anthranoids (Fig. 1), except hypericin and pseudohypericin (Fig. 2), were from commercial sources and were purchased from Carlo Erba (Milan, Italy), Extrasynthese (Genay, France), Merck (Darmstadt, Germany), Sigma–Aldrich (Milan, Italy). Purity of the compounds ($\geqslant$98%) was confirmed by NMR analysis. Hypericin and pseudohypericin were isolated from a commercial source of *Hypericum perforatum* L. (a gift of Indena, Milan, Italy) using the chromatographic methods according to Karioti et al.[29] Both identification and purity of hypericin and pseudohypericin ($\geqslant$98%) was checked by HPLC and NMR. All other reagents were of the highest purity available and obtained from commercial sources.

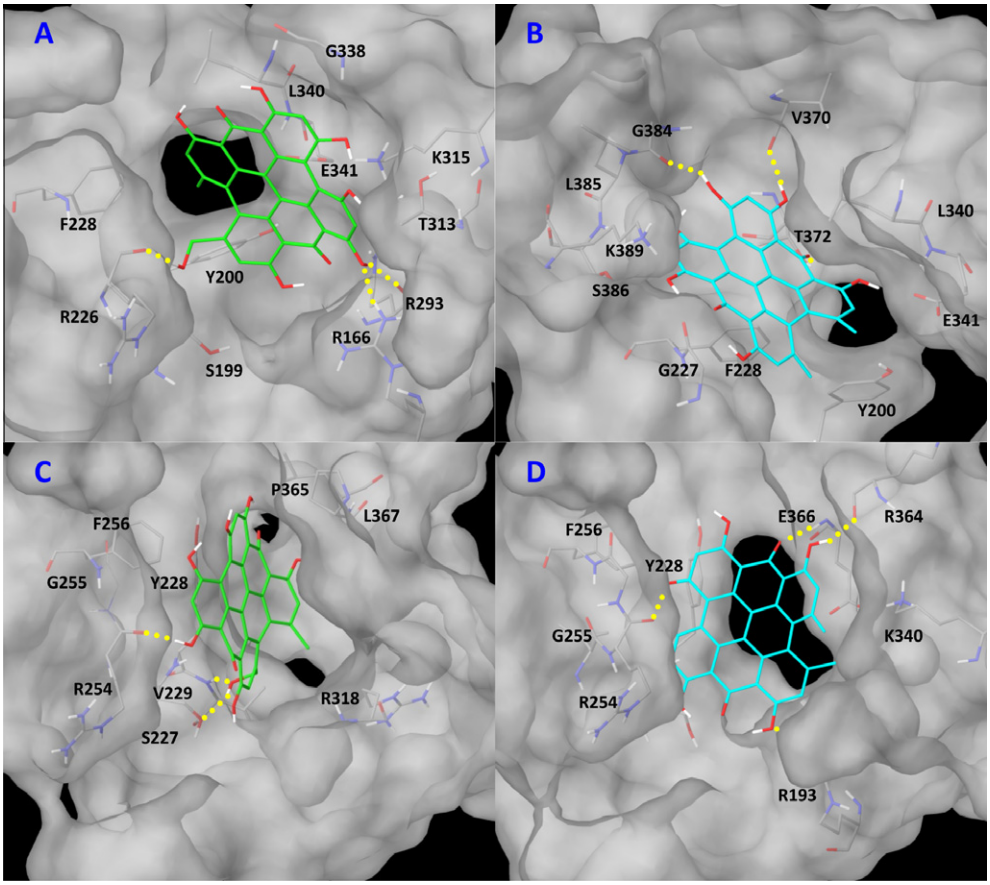

Figure 9. MMGB/SA relaxed poses of HYP and PHYP in TrxR1 (A and B) and in TrxR2 (C and D). Ligand molecules are shown in stick representation (green and cyano carbon atoms for PHYP and HYP, respectively). Only residues forming H-bond (yellow dashed lines) and in good van der Waals contacts with the ligands are reported, for clarity.

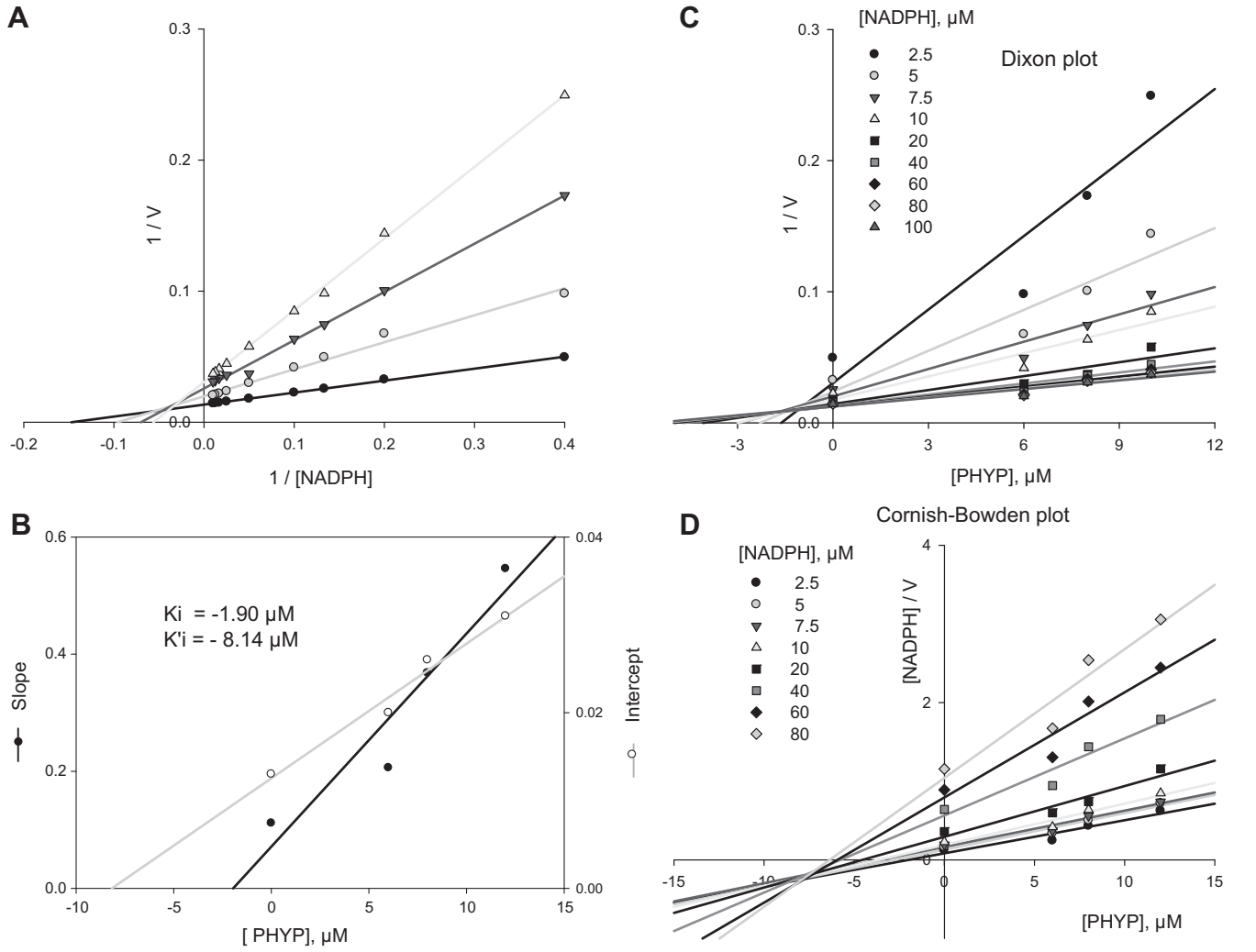

Figure 10. Inhibition kinetics of pseudohypericin on thioredoxin reductase**.** Measurements were performed at 25 °C in 0.2 M Na, K-Pi buffer (pH 7.4) containing 5 mM EDTA, 6.3 nM TrxR1 and increasing concentrations of NADPH (from 2.5 to 100 µM). Reactions were started by the addition of 1 mM DTNB and followed spectrophotometrically at 412 nm. In (A) concentrations of PHYP were (●) 0, (○) 6, (▼) 8 and (Δ) 12 µM. (B) shows slopes and intercepts obtained from (A) and plotted against PHYP concentrations. (C) and (D) are the Dixon and Cornish-Bowden plots, respectively. Symbols in (C) and (D) indicate the concentration (µM) of NADPH.

Table 2
Effect of anthraquinones on cytosolic and mitochondrial thioredoxin reductase

Compound	IC_{50} (µM)	
	TrxR1	TrxR2
Anthrone	>200	>200
1,4 Dihydroxyanthroquinone	>200	>200
1,8 Dihydroxyanthroquinone	>200	>200
Chrysophanol	194	181
Aloe emodin	180	>200
Aloin A	>200	>200
Rhein	84	123
Physcion	185	132
Sennosid A, B	>200	>200
Frangulin A	>200	>200
Skyrin glucoside	>200	>200
Hypericin	198	49
Pseudohypericin	4.6	7.9

Cytosolic (TrxR1) and mitochondrial (TrxR2) thioredoxin reductase (2–3 µg/ml) were incubated with increasing concentrations of the indicated anthranoid for 5 min at 25 °C in 0.2 M Na, K-phosphate buffer (pH 7.4) containing 0.25 mM NADPH and 2 mM EDTA. Reactions were started by the addition of 1 mM DTNB and followed spectrophotometrically at 412 nm.

4.2. Enzyme preparation and estimation

Cytosolic thioredoxin reductase (TrxR1) was isolated from rat liver according to Luthman and Holmgren.[30] Mitochondrial thioredoxin reductase (TrxR2) was prepared utilizing mitochondria isolated from rat liver according to Rigobello et al.[31] Glutathione reductase from yeast was purchased from Sigma. The protein content of purified enzymes was measured according to Lowry et al.[32] Thioredoxin reductase activity was estimated with the DTNB method or the insulin method.[30,33] Thioredoxin reductase was also measured by directly adding oxidized Trx in the absence of insulin in the same experimental conditions used with the insulin method. The oxidized status of Trx was controlled by the DTNB test. Glutathione reductase activity was estimated following the oxidation of NADPH in the presence of GSSG.

4.3. Labeling of thioredoxin reductase with BIAM[34]

TrxR1 (0.120 mg/ml) was pre-reduced with 130 µM NADPH in 10 mM Tris–HCl buffer (pH 7.4) containing 1 mM EDTA. Afterwards, 50 or 100 µM hypericin or pseudohypericin were added in

a final volume of 15 μl and the reaction carried out for 1 h at 25 °C. Aliquots (3 μl) were treated with 20 μM BIAM in a final volume of 20 μl of 0.2 M Hepes–Tris at pH 6.5 for 15 min at 37 °C. The reaction was blocked by adding a freshly prepared iodoacetamide solution (final concentration 50 mM). Samples were treated with 10 μl of loading buffer containing 0.1 M DTT and heated at 100 °C for 10 min, subjected to SDS–PAGE (7.5%) and then transferred to a nitrocellulose membrane. The biotinyl carboxamido methyl labeled proteins were detected by HRP-conjugated streptavidine followed by ECL.

4.4. Modeling/docking

All calculations were performed on 2xAMD Opteron285 Dual Core processor running Linux RedHat OS. Docking simulations were performed with Glide software (Grid-based Ligand Docking from Energetics)[35,36] and relied on the X-ray solved crystal structure of TrxR1 and TrxR2 both determined 3.0 Å resolution (1h6v and 1zdl code in the Protein Data Bank, respectively). The dimer formed by chains E and F of 1h6v was considered due to the higher number of solved residues of EF subunits with respect to AB and CD. Because 1zdl TrxR2 crystal structure contains a single subunit of the dimeric enzyme in the asymmetric unit, the dimer was rebuilt using the symmetry operation as indicated in PDB file. Both TrxR1 and TrxR2 dimers were prepared according to the recommended Protein Preparation Wizard in Maestro v8.5 in the presence of FAD and NADP. This procedure allowed to remove water molecule, to assign missing hydrogen atoms, to optimize protein's hydrogen bond network and to reduce structural problems. The default input parameters (no scaling factor for the vdW radii of non polar protein atoms, 0.8 scaling factor for non polar ligand atoms) were used and ligands docked using Glide's standard precision (SP) scoring function. Ligands pre-positioned with respect to 1zdl and 1h6v by docking procedure were relaxed, in turn, with the receptor, defining as flexible region all residues within 8 Å from the processed ligand while keeping all other protein atoms frozen using Prime[36] Three-dimensional structures of hypericin and pseudohypericin were modeled using the LigPrep Schrödinger ligand preparation procedure (pH 7.4) and minimized with Macromodel 9.0 (available from Schrödinger).[36]

Supplementary data

Supplementary data associated with this article can be found, in the online version, at doi:10.1016/j.bmc.2010.10.045.

References and notes

1. Lown, J. W. *Chem. Soc. Rev.* **1993**, *22*, 165.
2. Abad Martínez, M. J.; Bermejo Benito, P. *Stud. Nat. Prod. Chem.* **2005**, *30*, 303.
3. Tulp, M.; Bohlin, L. *Bioorg. Med. Chem.* **2005**, *13*, 5274.
4. Kubin, A.; Wierrani, F.; Burner, U.; Alth, G.; Grünberger, W. *Curr. Pharm. Des.* **2005**, *11*, 233.
5. Bilia, A. R.; Gallori, S.; Vincieri, F. F. *Life Sci.* **2002**, *70*, 3077.
6. Kiesslich, T.; Krammer, B.; Plaetzer, K. *Curr. Med. Chem.* **2006**, *13*, 2189.
7. Johnson, S. A. S.; Pardini, R. S. *Free Radical Biol. Med.* **1998**, *24*, 817.
8. Frew, T.; Powis, G.; Berggren, M.; Abraham, R. T.; Ashendel, C. L.; Zalkov, L. H.; Hudson, C.; Qazia, S.; Gruszecka-Kowalik, E.; Merriman, R.; Bonjouklian, R. A. *Anticancer Res.* **1994**, *14*, 2425.
9. Agostinis, P.; Vandenbogaerde, A.; Donella-Deana, A.; Pinna, L. A.; Lee, K. T.; Goris, J.; Merlevede, W.; Vandenheede, J. R.; de Witte, P. *Biochem. Pharmacol.* **1995**, *49*, 1615.
10. Zhong, L.; Arnér, E. S. J.; Ljung, J.; Åslund, F.; Holmgren, A. *J. Biol. Chem.* **1998**, *273*, 8581.
11. Gromer, S.; Urig, S.; Becker, K. *Med. Res. Rev.* **2004**, *24*, 40.
12. Lyne, P. D.; Lamb, M. L.; Saeh, J. C. *J. Med. Chem.* **2006**, *49*, 4805.
13. Still, W. C.; Tempczyk, A.; Hawley, R. C.; Hendrickson, T. *J. Am. Chem. Soc.* **1990**, *112*, 6127.
14. Gromer, S.; Arscott, L. D.; Williams, C. H., Jr.; Schirmer, R. H.; Becker, K. *J. Biol. Chem.* **1998**, *273*, 20096.
15. Arnér, E. S. J.; Holmgren, A. *Eur. J. Biochem.* **2000**, *267*, 6102.
16. Urig, S.; Becker, K. *Semin. Cancer Biol.* **2006**, *16*, 452.
17. Fang, J.; Lu, J.; Holmgren, A. *J. Biol. Chem.* **2005**, *280*, 25284.
18. Lu, J.; Papp, L. V.; Fang, J.; Rodriguez-Nieto, S.; Zhivotovsky, B.; Holmgren, A. *Cancer Res.* **2006**, *66*, 4410.
19. Du, Y.; Wu, Y.; Cao, X.; Cui, W.; Zhang, H.; Tian, W.; Ji, M.; Holmgren, A.; Zhong, L. *Biochimie* **2009**, *91*, 434.
20. Cenas, N.; Nivinskas, H.; Anusevicius, Z.; Sarlauskas, J.; Lederer, F.; Arnér, E. S. J. *J. Biol. Chem.* **2004**, *279*, 2583.
21. Ravi, D.; Das, K. C. *Cancer Chemother. Pharmacol.* **2004**, *54*, 449.
22. Witte, A. B.; Anestål, K.; Jerremalm, E.; Ehrsson, H.; Arnér, E. S. J. *Free Radical Biol. Med.* **2005**, *39*, 696.
23. Huang, Q.; Lu, G.; Shen, H.-M.; Chung, M. C. M.; Ong, C. N. *Med. Res. Rev.* **2007**, *27*, 609.
24. Rigobello, M. P.; Messori, L.; Marcon, G.; Cinellu, M. A.; Bragadin, M.; Folda, A.; Scutari, G.; Bindoli, A. *J. Inorg. Biochem.* **2004**, *98*, 1634.
25. Rigobello, M. P.; Scutari, G.; Boscolo, R.; Bindoli, A. *Br. J. Pharmacol.* **2002**, *136*, 1162.
26. Vandenbogaerde, A. L.; Kamuhabwa, A.; Delaey, E.; Himpens, B. E.; Merlevede, W. J.; de Witte, P. A. *J. Photochem. Photobiol., B: Biol.* **1998**, *45*, 87.
27. Agostinis, P.; Donella-Deana, A.; Cuveele, J.; Vandenbogaerde, A.; Sarno, S.; Merlevede, W.; de Witte, P. *Biochem. Biophys. Res. Commun.* **1996**, *220*, 613.
28. Berndt, C.; Lillig, C. H.; Holmgren, A. *Am. J. Physiol. Heart Circ. Physiol.* **2007**, *292*, H1227.
29. Karioti, A.; Vincieri, F. F.; Bilia, A. R. *J. Sep. Sci.* **2009**, *32*, 1374.
30. Luthman, M.; Holmgren, A. *Biochemistry* **1982**, *21*, 6628.
31. Rigobello, M. P.; Callegaro, M. T.; Barzon, E.; Benetti, M.; Bindoli, A. *Free Radical Biol. Med.* **1998**, *24*, 370.
32. Lowry, O. H.; Rosebrough, N. J.; Farr, A. L.; Randall, R. J. *J. Biol. Chem.* **1951**, *193*, 265.
33. Holmgren, A. *Methods Enzymol.* **1984**, *107*, 295.
34. Chew, E.-H.; Lu, J.; Bradshaw, T. D.; Holmgren, A. *FASEB J.* **2008**, *22*, 2072.
35. Friesner, R. A.; Banks, J. L.; Murphy, R. B.; Halgren, T. A.; Klicic, J. J.; Mainz, D. T.; Repasky, M. P.; Knoll, E. H.; Shelley, M.; Perry, J. K.; Shaw, D. E.; Francis, P.; Shenkin, P. S. *J. Med. Chem.* **2004**, *47*, 1739.
36. Schrödinger, L.L.C., New York, 2005. (http://www.schrodinger.com).